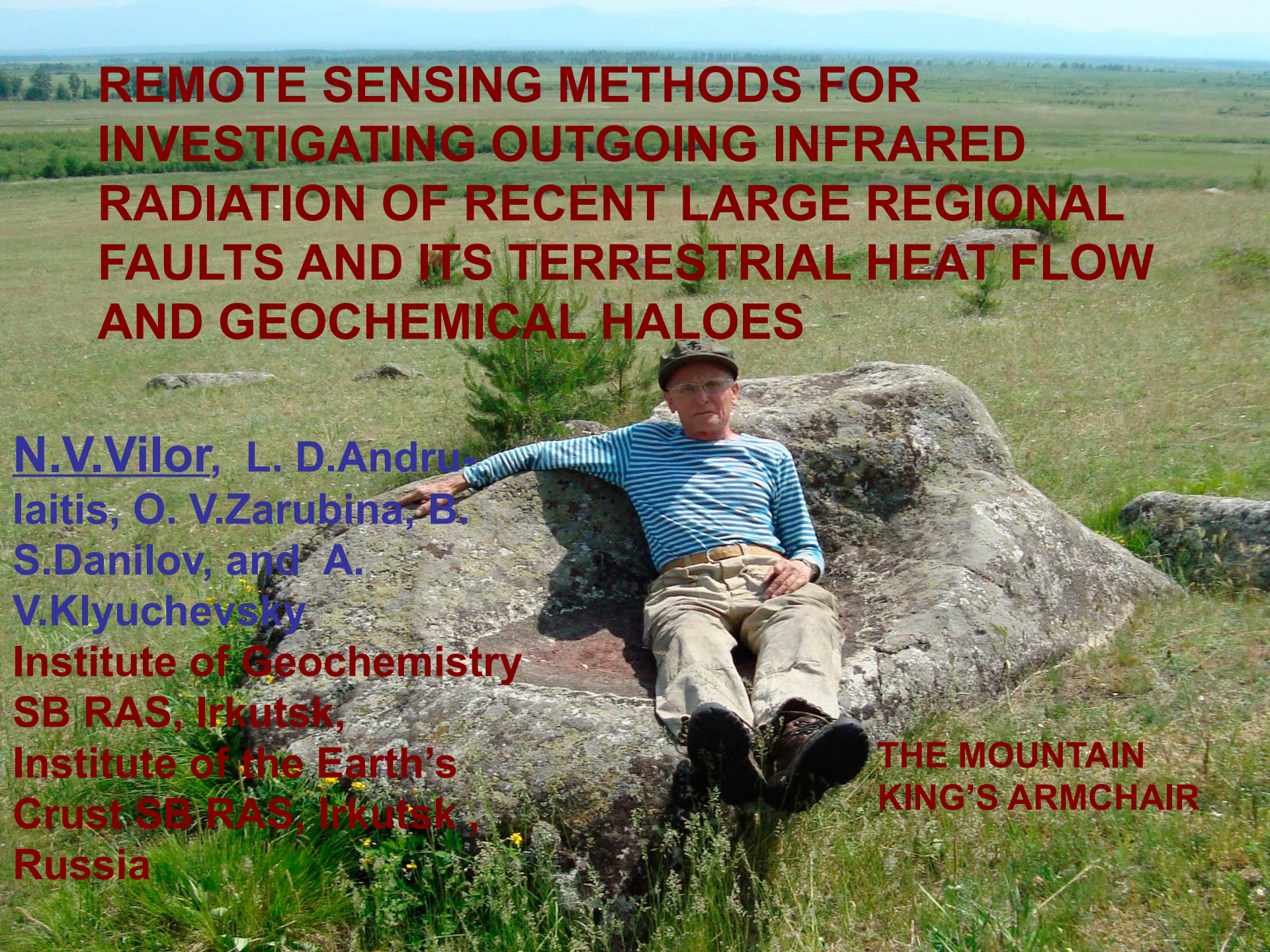


REMOTE SENSING METHODS FOR INVESTIGATING OUTGOING INFRARED RADIATION OF RECENT LARGE REGIONAL FAULTS AND ITS TERRESTRIAL HEAT FLOW AND GEOCHEMICAL HALOES

N.V.Vilor, L. D.Andru-
laitis, O. V.Zarubina, B.
S.Danilov, and A.
V.Klyuchevsky

Institute of Geochemistry
SB RAS, Irkutsk,
Institute of the Earth's
Crust SB RAS, Irkutsk,
Russia

THE MOUNTAIN
KING'S ARMCHAIR

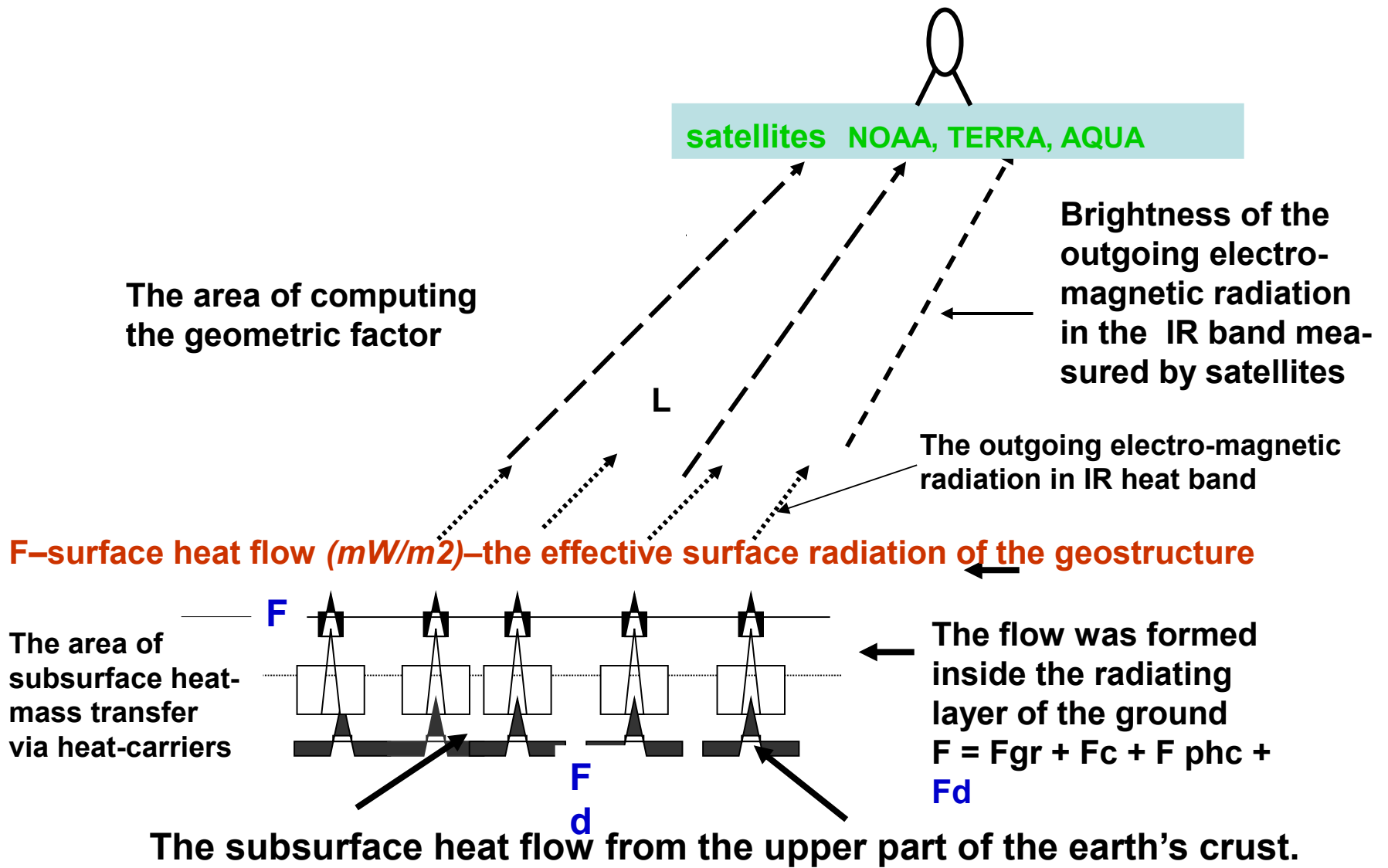


Purpose

· Determination of intensity of outgoing IR radiation flow of large seismoactive regional faults, which are exposed by surface heat flows by remote sensing method and correlation this flow with transfer of mobile chemical elements and its geochemical flows

Items

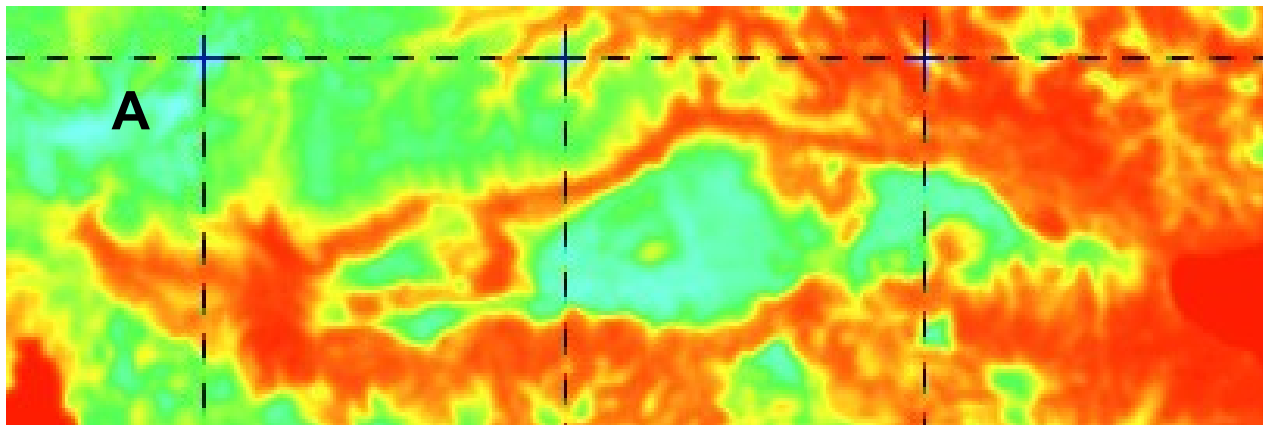
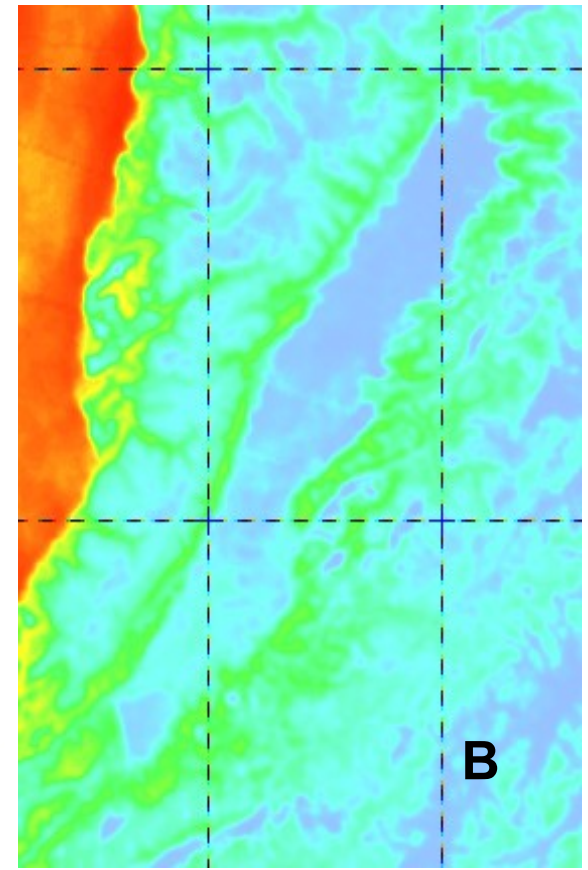
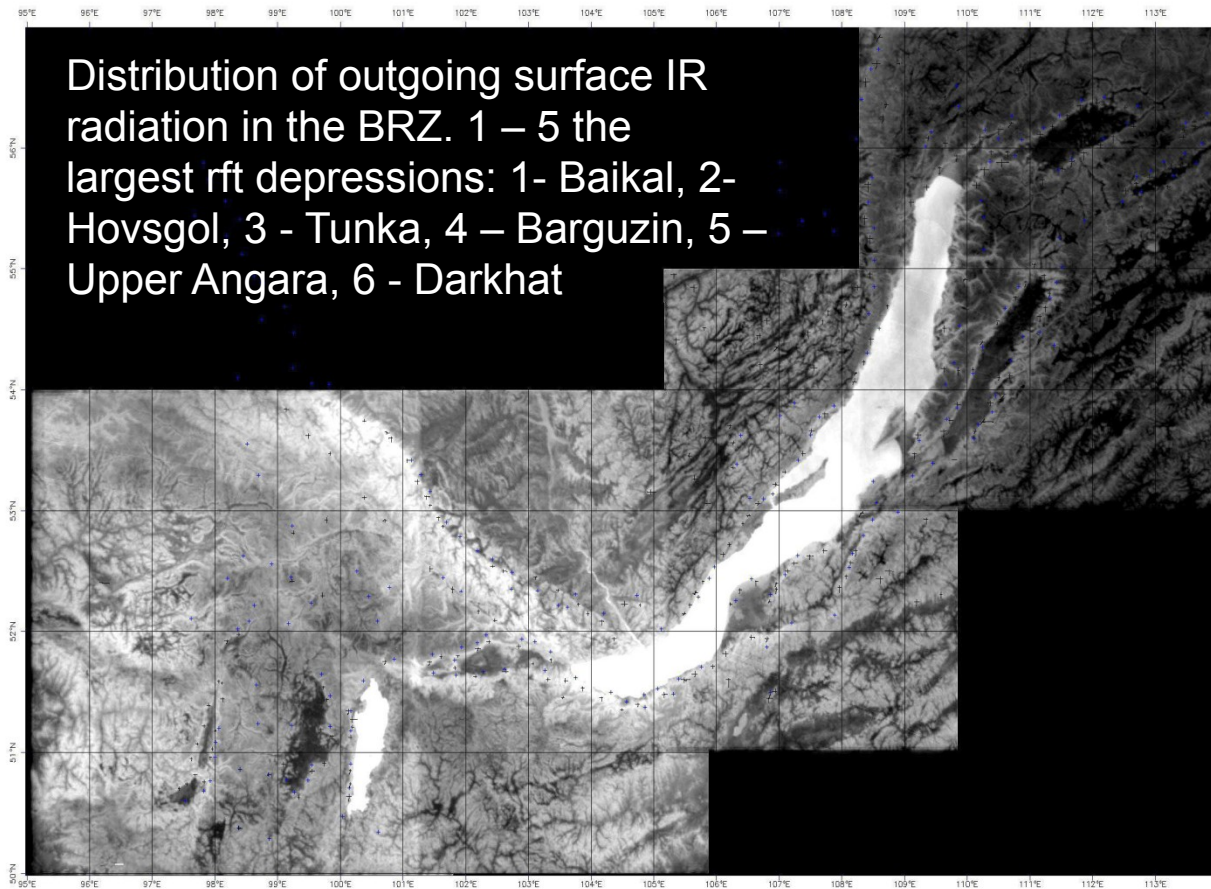
- the remote sensing method of mapping of distribution of intensity of outgoing IR radiation flow for different geodynamic situation_
- the investigation of nature of surface outgoing IR radiation flow_
- the investigation of distribution of mobile chemical elements into surface formations of regional faults _
- the calculation of its geochemical flows by using the conception of geochemical barriers



THE SCHEME OF THE ORIGIN OF THE SURFACE INFRARED RADIATION OF THE LARGE REGIONAL FAULTS

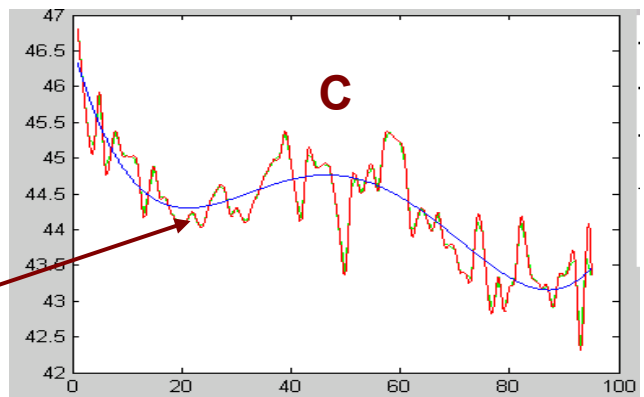
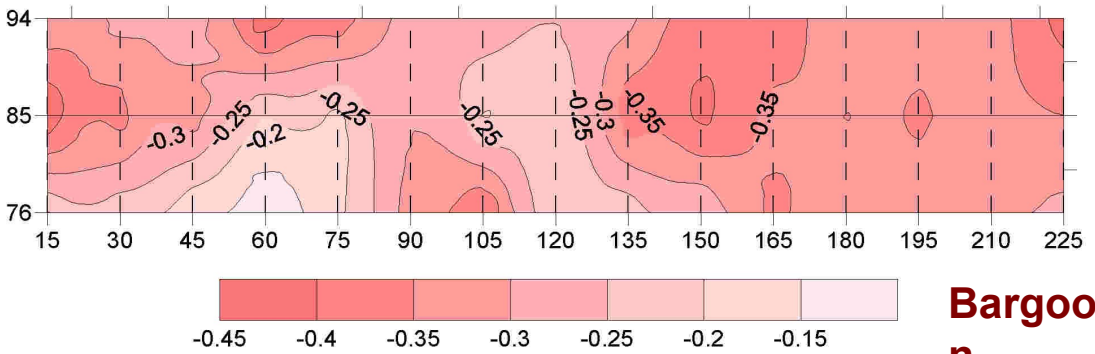
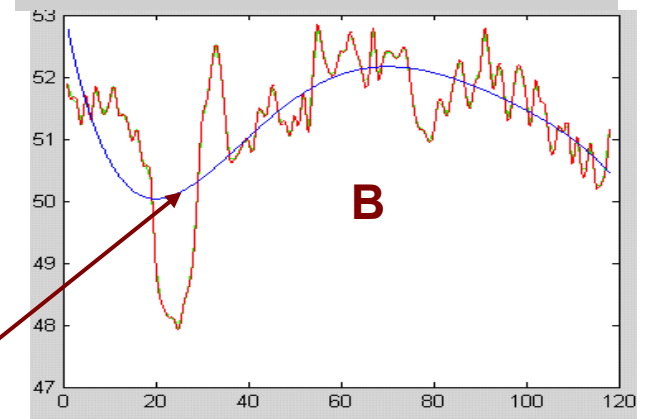
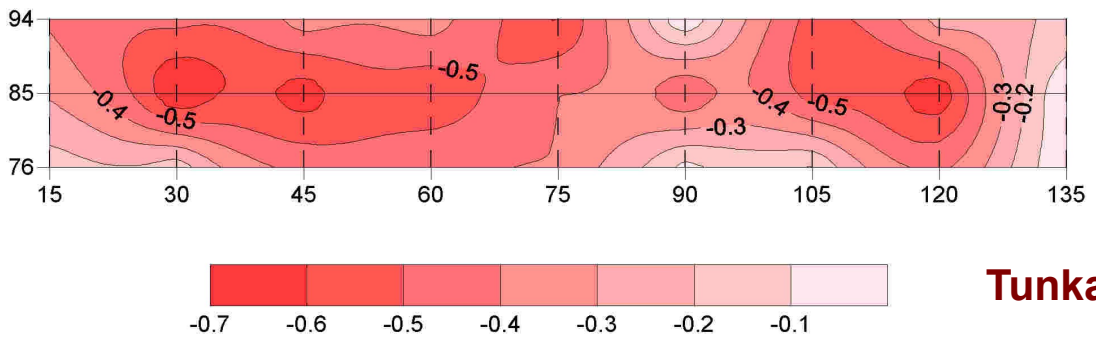
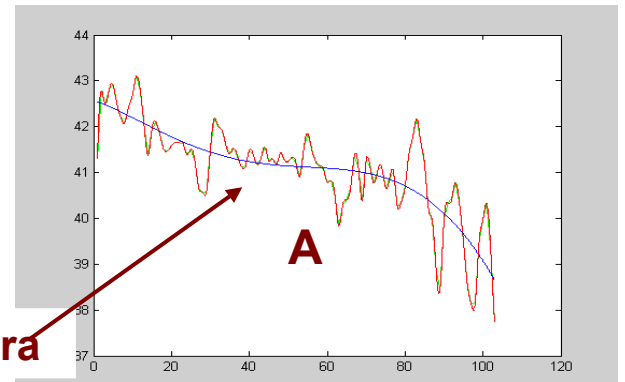
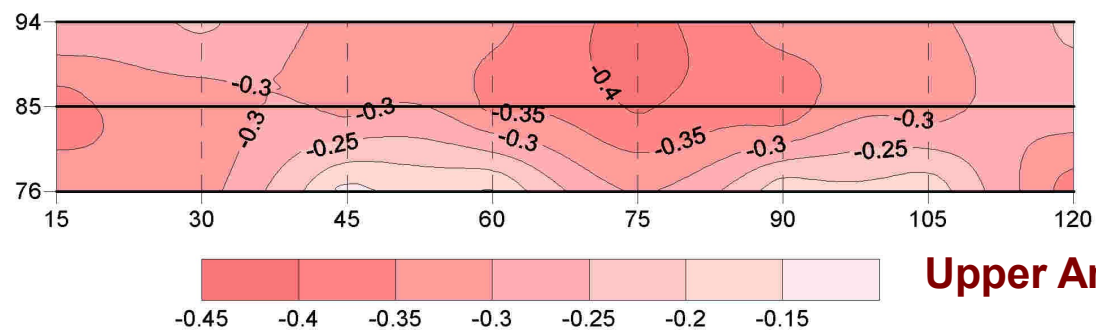
Geodynamical situations of manifestation of outgoing surface IR radiation flow of large seismoactive regional fault

Type of regional deformation	Region
Tention, rifting	Baikal rift zont (BRZ), Rhine graben, “Afar triangle” + Eastern – African rift
Displacement	San – Andreas transform fault system
Collision	Himalayas, Western- Copetdag structural arc
Block compression, ramp situation	Tarim basin and its folded frame

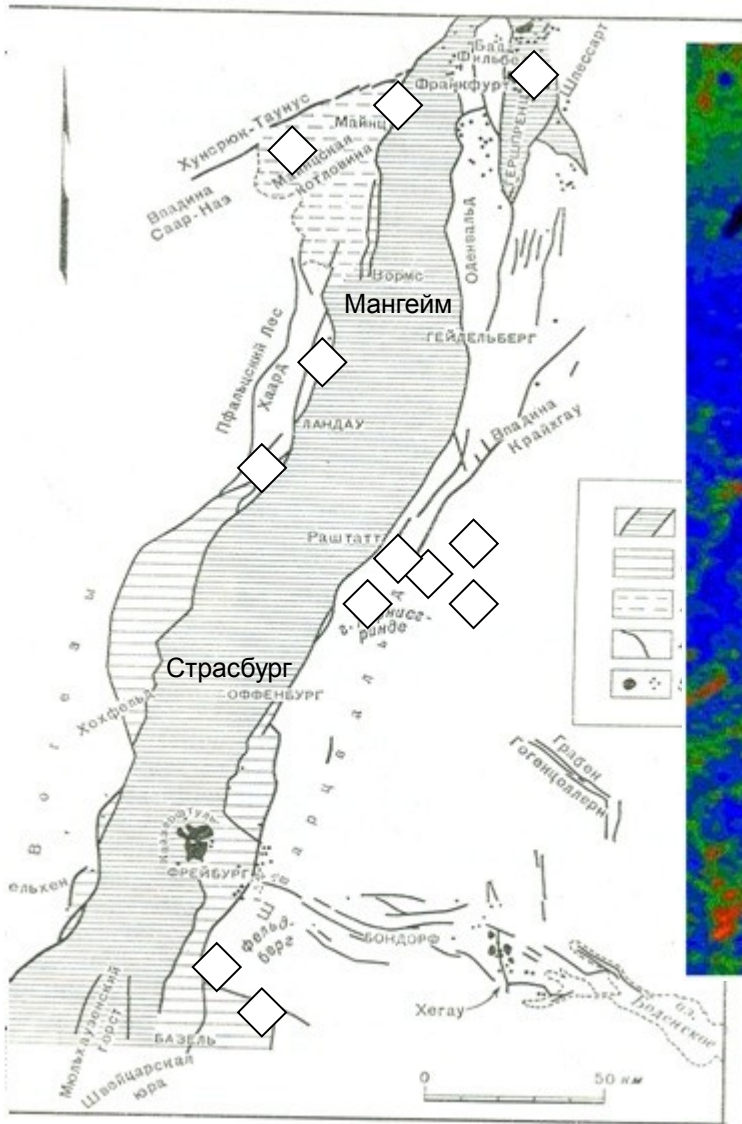


Rift situation.
 Outgoing surface IR flow large tectonic depressions BRZ.
A. Tunka depression. **B.** Bargoozin depression.

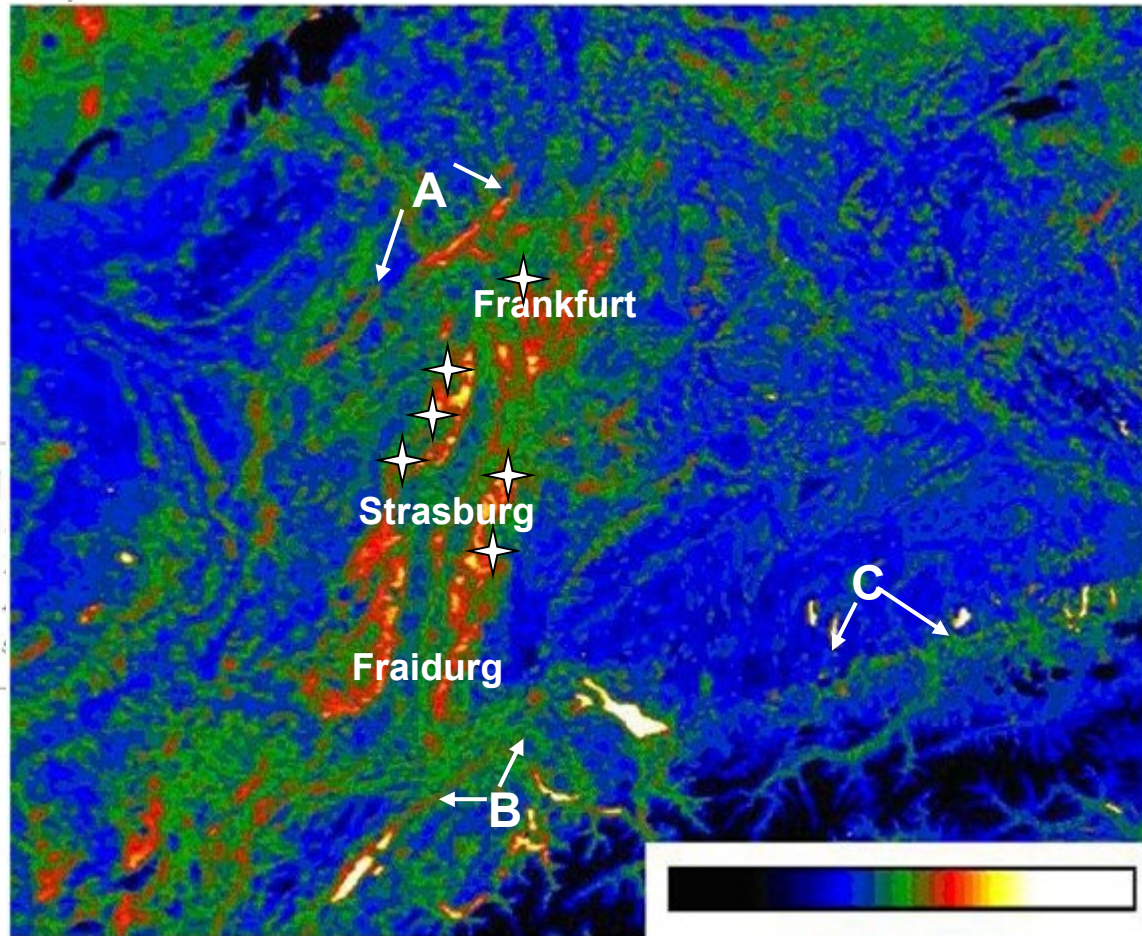
The temporal maps of regional permeability along large faults BRZ for 1976 – 1994 years



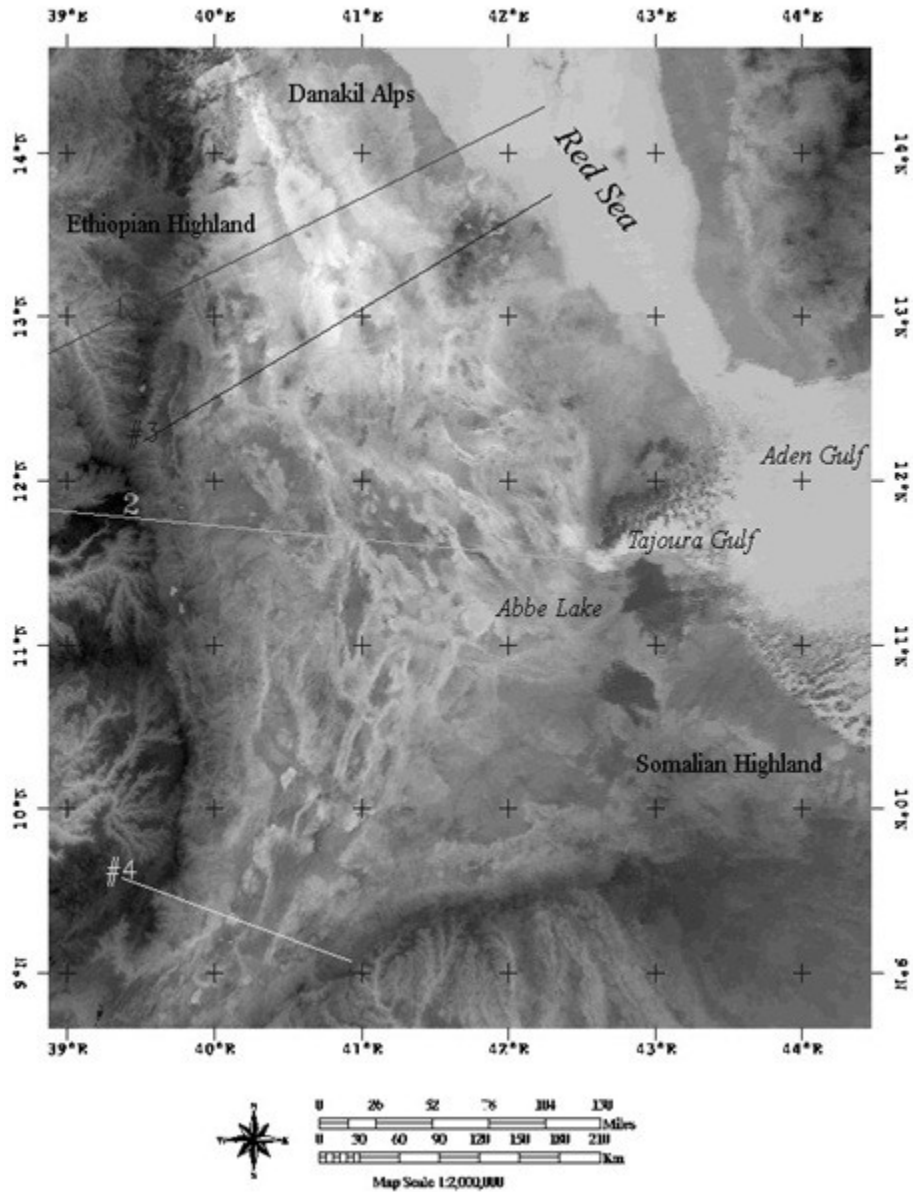
The low length wave of geometric component of plots of outgoing surface IR flows of BRZ' largest faults



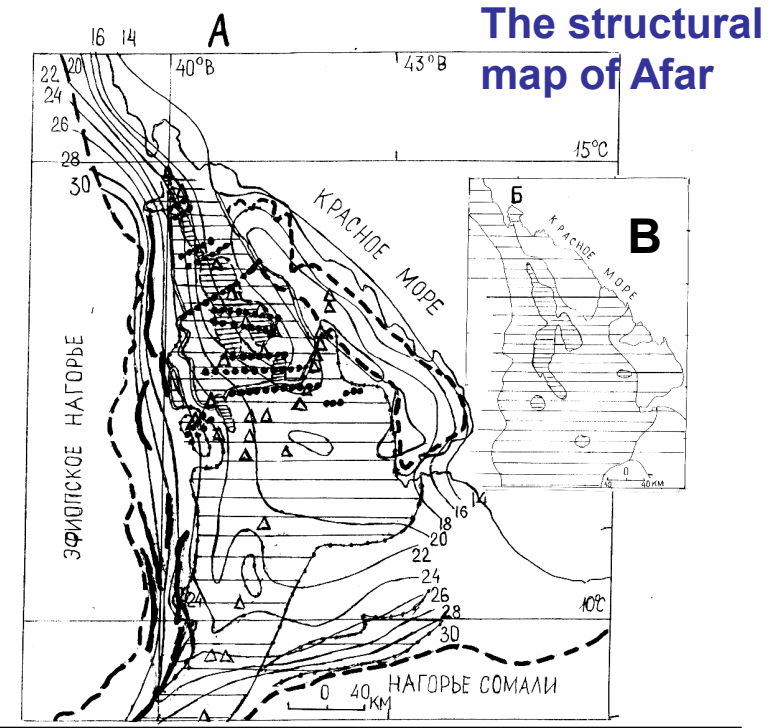
The structural map of Rhine graben. thermal water springs (after Friedrichsen, 1981)



Outgoing surface IR flows map of Western Europe part with Rhine graben. A, B, C – large regional faults (after Gorni V.I. 2007)
 ✦ famous water spring

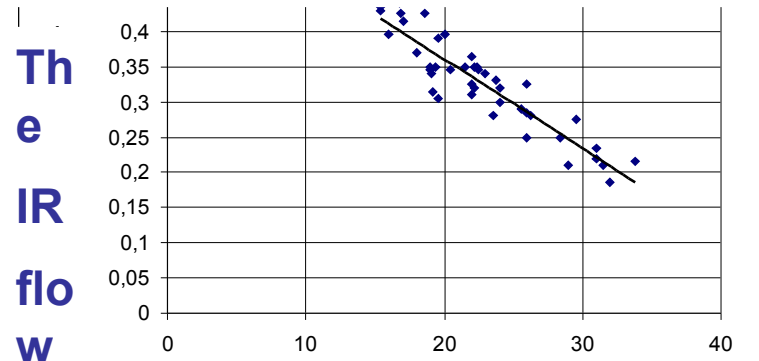


The outgoing surface IR flow map of Afar depression and mouth of Eastern African rift



The structural map of Afar

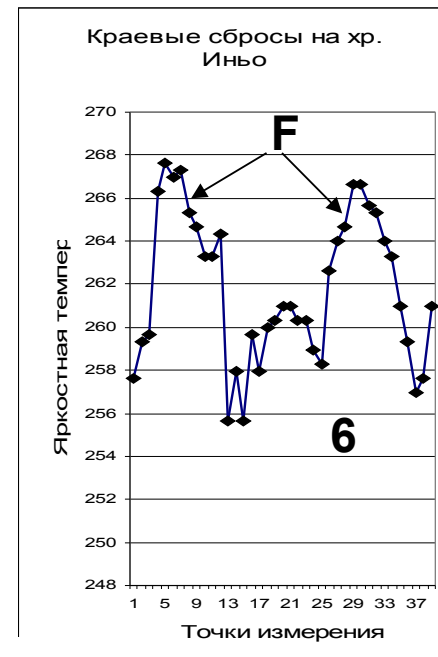
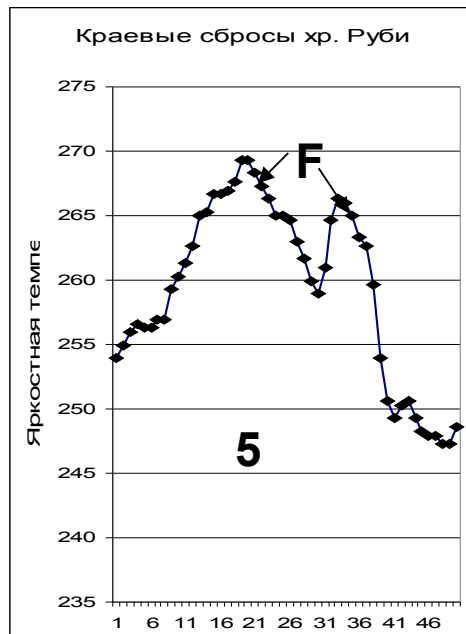
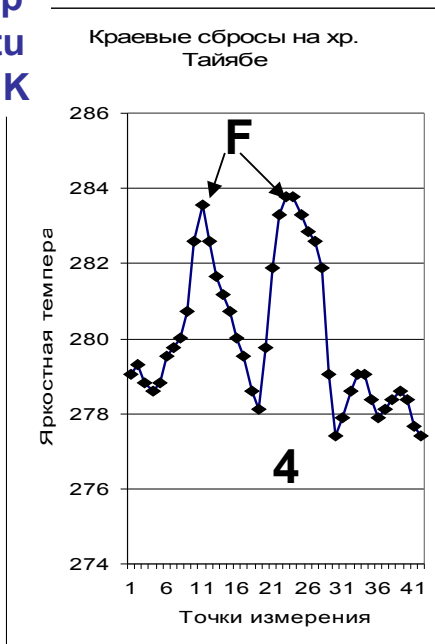
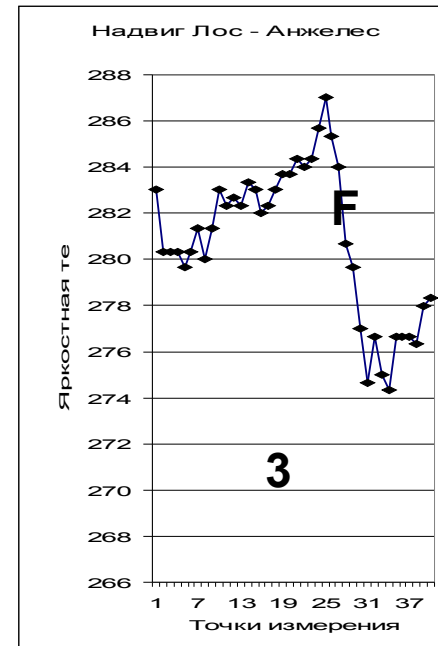
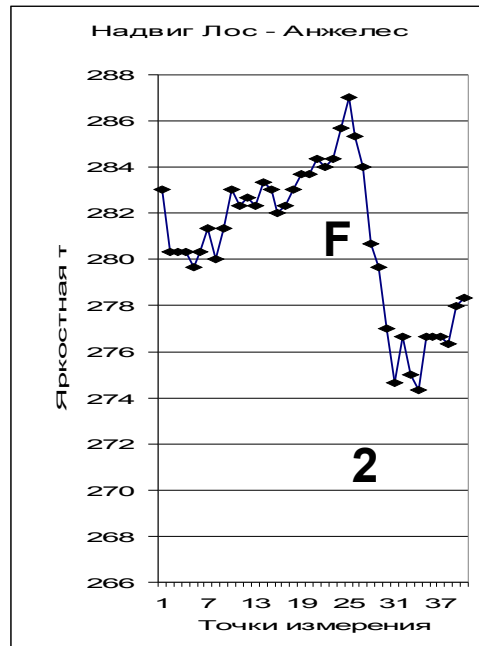
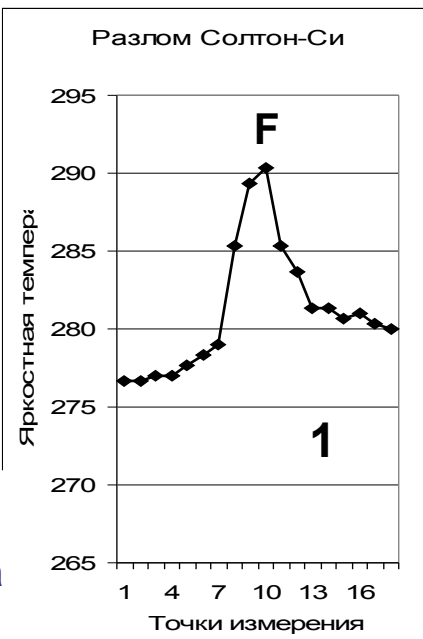
The correlation of the depth of bedding of Moho surface and outgoing IR flow



The
e
IR
flo
w

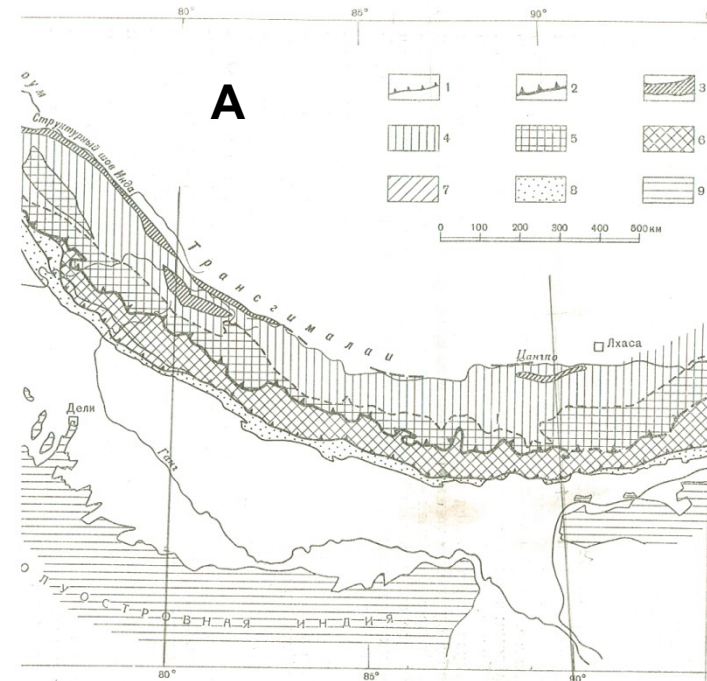
The depth of bedding of Moho surface, km

IR
radiation
temperature, K

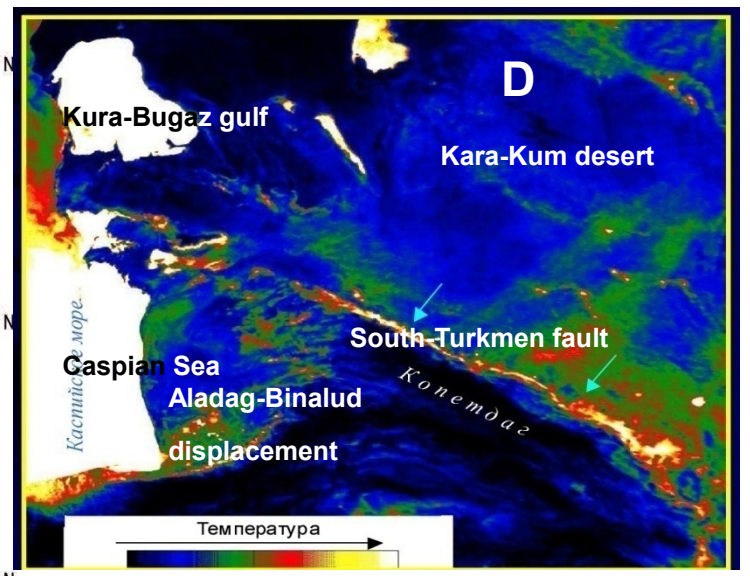
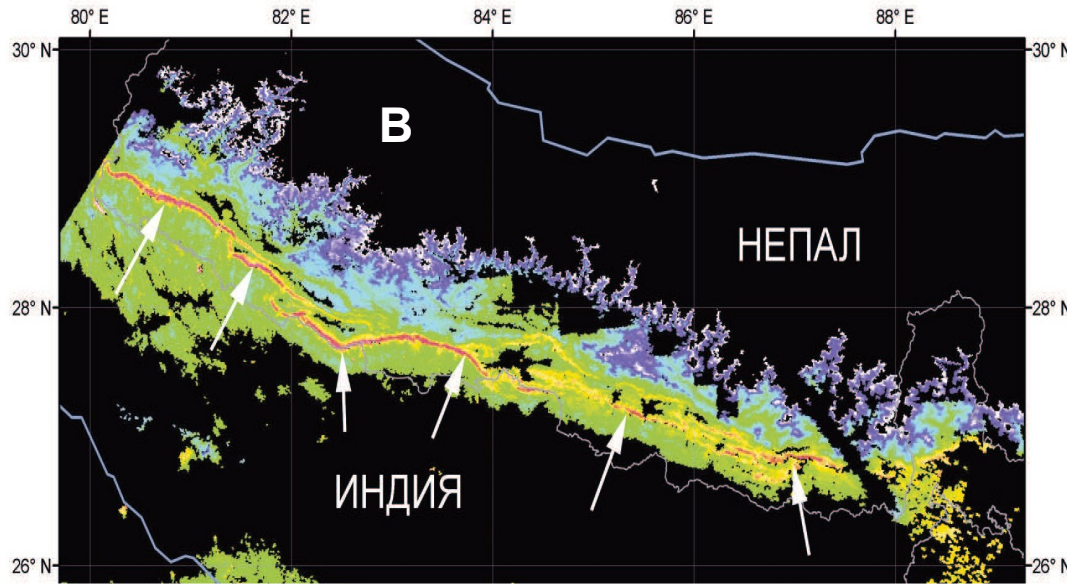
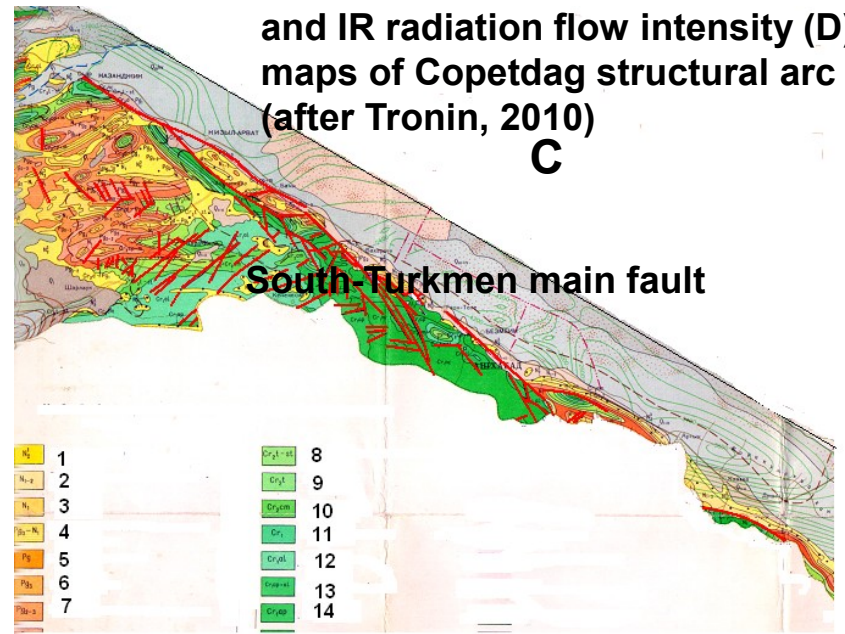


IR
radiation
anomalies
of the
surface of
large
faults of
San
Andreas
system
(1-3) and
on faults
of Big
Basin
province
(4-6) F –
fault's
tracks

Points of dimension

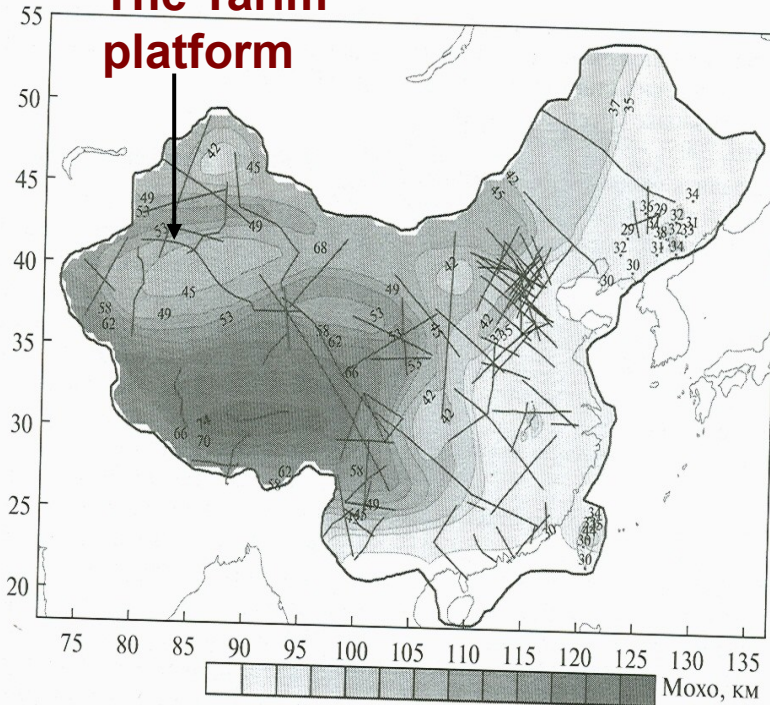


Collision situation. Structural (C) and IR radiation flow intensity (D) maps of Copetdag structural arc (after Tronin, 2010)



Structural (A) and IR radiation flow intensity (B) maps of the main border

The Tarim platform

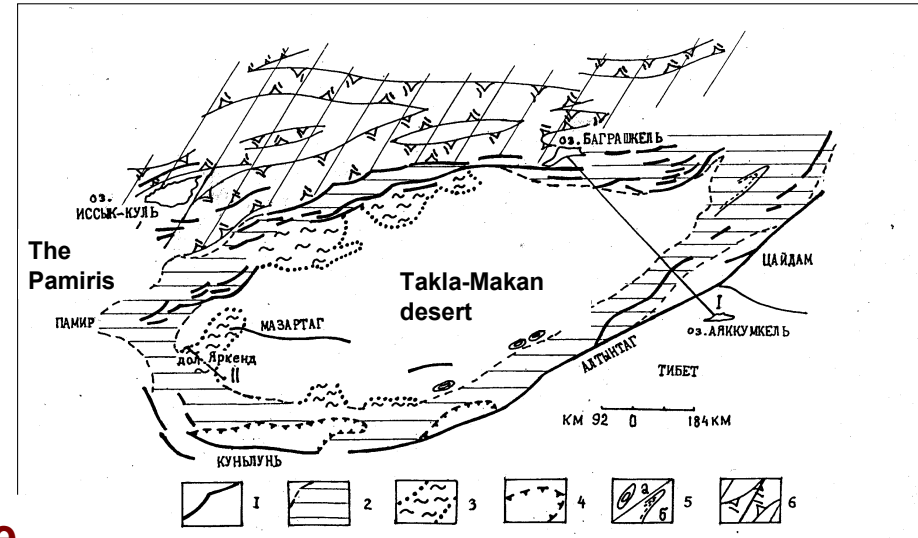


Remote sensing and investigation of leaving regional faults infrared radiation and its geophysical and geochemical components

Vilor Nikolay V., et.all



Fig.3 Location of regional faults on the Tarim platform and its folded margins, the compression structure



The new map of Moho surface for Chinese territory

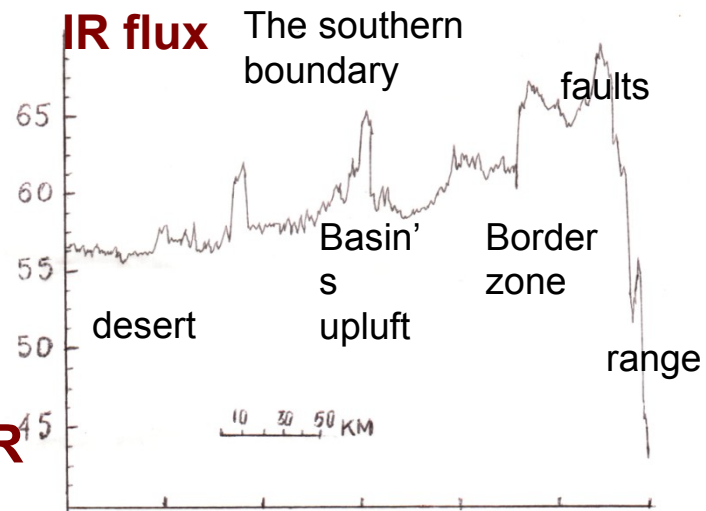
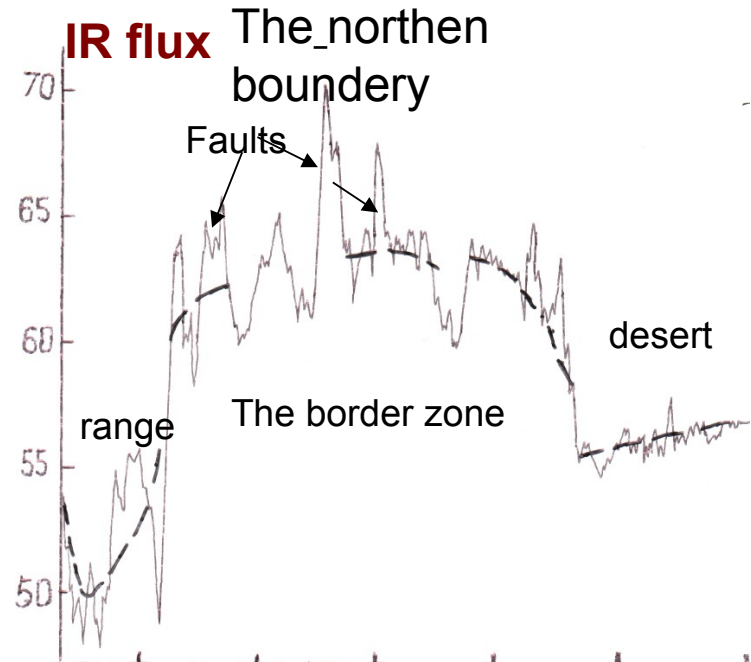
by Baranov, @Earth Physics, N1, 2009

Ramp situation

opes of the uplifted block of the upper crust, which corresponds to the massif of the Tarim platform.



Brightness of the contrast outgoing surface IR flow for the Tarim platform and its framing (January 2001, night)



The distance, km

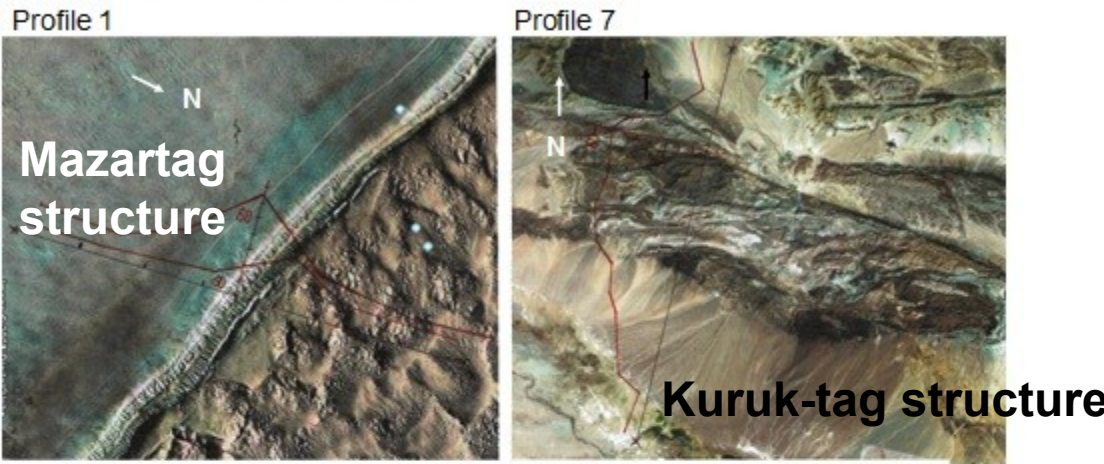
The distribution of IR flux intensity across Tarim platform

Remote sensing and investigation of leaving regional faults infrared radiation and its geophysical and geochemical components

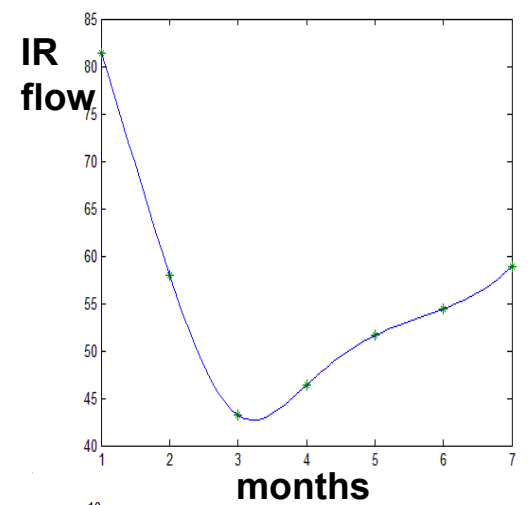
Vilor Nikolay V., et.all



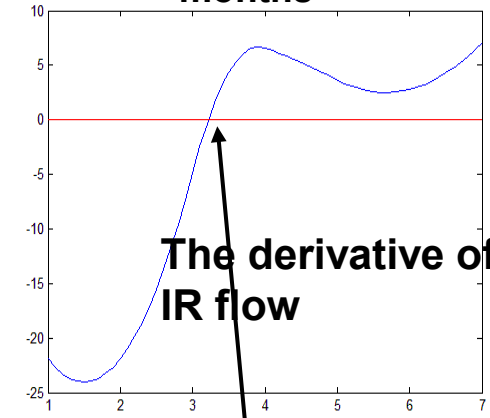
Distribution of outgoing surface IR flux on the elements of the Tarim platform geological structure on profiles 1 and 7. 1 is the center of the platform – Mazartag structure; 7 is the Upper Proterozoic uplift of the platform basement (Kuruktag)



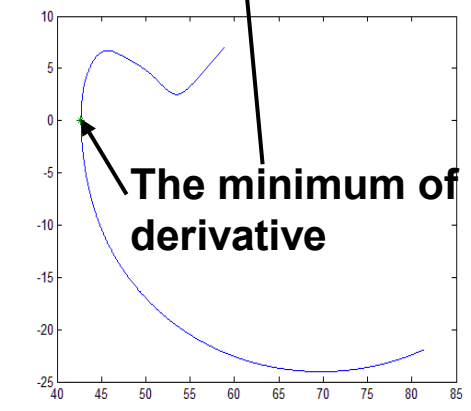
st. 48° 31' 3" n.lat, fin 39° 42' 22" n.lat, 80° 31' 13" st. 41° 20' 51" n.lat, fin. 40° 50' 8" n.lat, 87° 49' 39" e.



The calculation of quasistationary IR flow



The derivative of IR flow



The minimum of derivative

The calculated surface heat flow of large regional faults of BRZ

The transition to the values of brightness measured for the surface IR flow can be made with the use of the following relation

$$F = L \cdot G \quad (\text{Gossorg, 1980}) \quad (1),$$

where **F** - surface IR flow, **L** - brightness IR flow, **G** - geometric factor, which writes

$$G = \pi \cdot S \cdot \sin^2 \alpha = 6.8704 \quad (\text{m}^2 \cdot \text{ster}).$$

Hence the surface IR flow **F** computed by (1) makes: **F = 6.8704 L (mW)**.

Values of **F** are added for the components, which form its **balance**. The addends of such a balance include: **F_{gr}** – heat flow of the active ground layer (the result of heat inertia), **F_c** – heat effect of the surface condensation or crystallization of water vapor, **F_{pch}** – heat effect of the process of oxidation of gases coming from the ground in the upper part of the active layer, **F_d** – **component of the deep heat flow**. Hence, we have:

$$F = F_{gr} + F_c + F_{pch} + F_d$$

The sub-surface **endogenic flow F_d** is the sum of influences of the **conductive** and **the convective components** upon the radiating layer. The difference between the value of the near-surface endogenic flow **F_d** and the near-surface **conductive component F_{cnd}** computed represents the share of the **convective component**

$$F_{cnv} = F_d - F_{cnd}$$

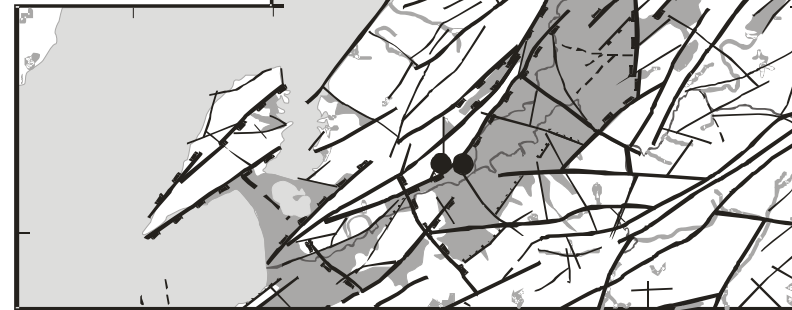
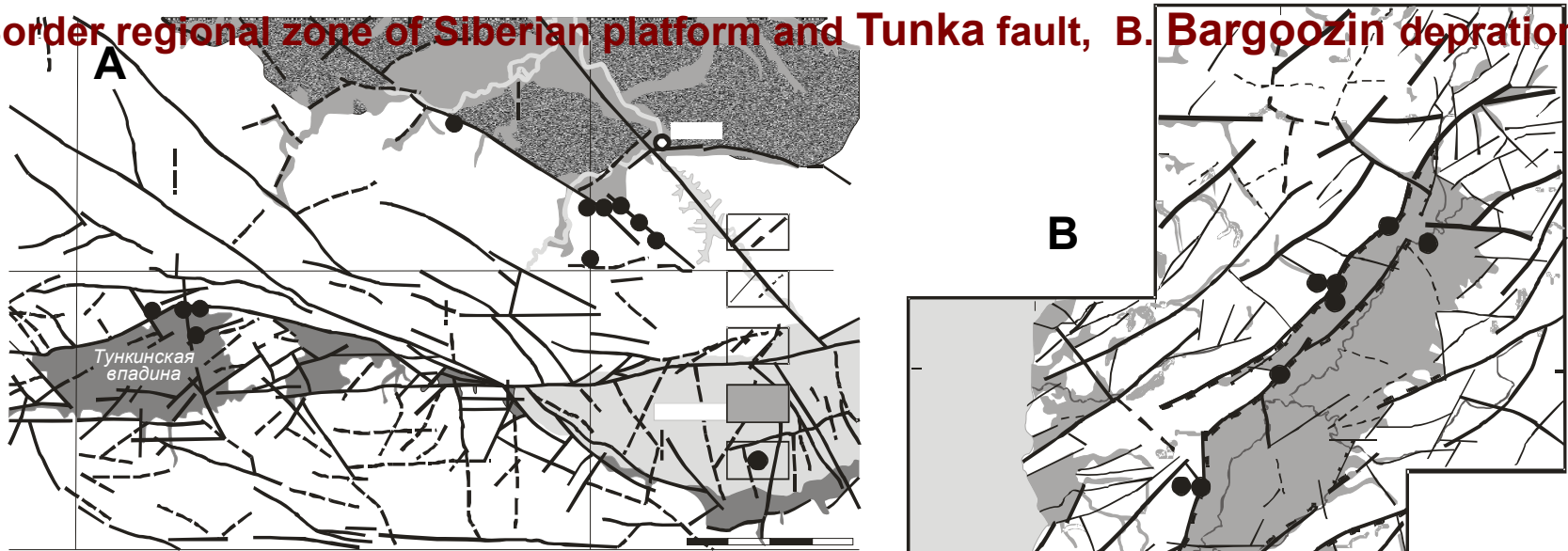
Fault	Brightness flow, <i>L</i> mW/m ² . cr.μm	Surface heat flow, <i>F</i> mW	Depth part of <i>F</i> , <i>F dep</i> , mW	Portion of <i>F depth</i> , mW		The part of konvektive portion, %
				konductive <i>F conda</i>	konvektive <i>F conve</i>	
Tunka	103.027	707.84	323.37	25.46±4.14	297.86±4.18	92
Bargoo ezun	85.466	587.19	362.14	25.44±2.69	336.71±2.7	93
Near-sea	112.242	771.15	339.36	20.94±1.67	318.42±1.67	94
Border zone of platf.	103.64	708.09	289.62	18.79±0.87	270.86±0.77	94

The calculated surface heat flow of large regional faults of Tarim basin and its folded frame

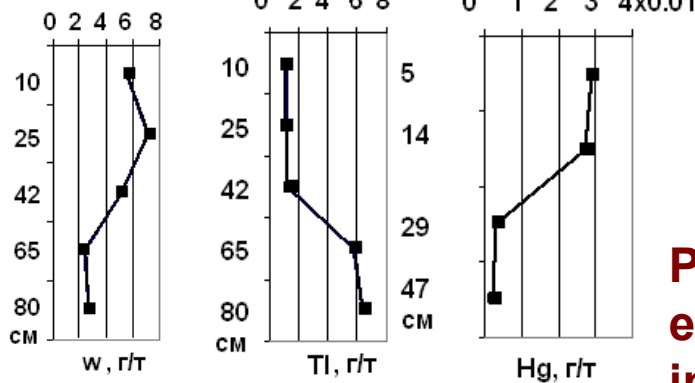
Fault structure	Surface heat flow <i>F</i> , mW	Depth conductive part of <i>F</i> , calculated	Portion of <i>F depth</i> , mW	
			konductive, <i>F conda</i>	konvektive, <i>F conve</i>
Mazartag	61.47	40	19.59	41..88 (68)
Kalpintag	196.56	40	19.59	176..97 (90)
Choltag	199.87	44	20.22	179..65 (90)
Kuruktag	186.86	45	20.38	166.48 (89.1)
Altuntag	256.56	43	20.06	236.48 (92)

The set of geochemical samples on large seismoactive regional fault's tracks of BRZ

A. Border regional zone of Siberian platform and Tunka fault, B. Bargoozin depression



Depth, cm



The concentration is g / t

Plots of volatile chemical ore element's concentration distribution into surface formations of Bargoozine regional fault

Geochemical indicators, associated with surface outgoing IR flow of large seismoactive faults of BRZ

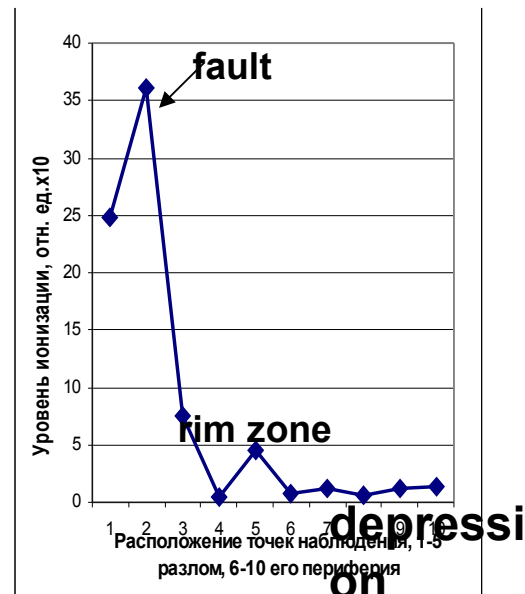
Fault	n	C m	B	Cu	Zn	Pb	As	Ge	Mo	Sn	Ag	Tl	Hg	Co	Cr	Ni	V
Tunka	88	X	42.	34.2	75.40	13.9	11.6	1.2	1.98	2.6	0.2	0.9	0.1	16.1	81	68	68.2
		±σ	2.0	1.32	1.12	1.31	1.62	0.4	1.35	0.9	0.2	1.0	0.1	1.3	1	1	1.3
Bargoozin	75	X c	14.3	25.9	112.1	17.9	6.14	1.2	1.55	3.1	0.2	0.7	0.1	16.7	51	39	95
		±σ	1.1	1.18	1.05	1.03	1.33	0.3	1.25	1.0	0.1	0.4	0.1	1.0	1	1	1
Border zone of platform	91	X	20.6	22.8	69.65	12.4	17.4	1.2	1.25	2.3	0.3	0.8	0.6	не определены			
		±σ	2.1	1.28	1.25	1.59	2.21	0.6	1.82	1.2	0.3	1.4	1.5				
Geotherm. field Kucheger		X	20.3	23.9	88.65	18.2	14.3	3.9	1.14	2.2	0.74	0.6	0.1	11.9	42	36	60.3
		±σ	1.1	1.33	1.19	1.1	1.61	1.7	1.09	1.1	1.5	0.4	0.2	1.1	1.1	1.2	1.1

Fault	Indicators of geochemical specialization of faults						
	High concentration, g / t		According to dispersion		According to geochemical association		
	Cmax	Back-ground	9 elements F1/F2	15 elements, F1/F2	9 elements	15 elements	Main / secondary
Tunka	B, Cu, Cr	B, Cu	Ge, B / Tl, Mo	B / Mo	Tl, Ag, Mo, B	Hg, As, Ag, Mo	Ag, Mo / Hg, As, Tl
Bargoozin	Zn, V	Zn, V	Ag, Cu / Pb, Tl	Ni, As / Pb, Mo	Tl, Cu, Ag,	Mo, As, Tl	Tl / Cu, Ag, As
Border zone of platform	As, Hg	Hg	Cu, Zn / Tl, Mo	Mo, As / Zn	Mo, Tl, Ag	Mo, Hg, As, Ag	Mo, Ag / Tl, Hg, As,
Geothermal field Kucheger	Ge, Ag	Ge, Ag	не рассчитано	Zn, Pb / V, Co	не рассчит.	Hg, Ag, Mo, Ge	Hg, Ag, Ge / Mo

Π , geochim. flow = $[C \text{ comp} : (S \cdot t)] \cdot 10^6 = \text{kg/km}^2 \cdot \text{year}$.

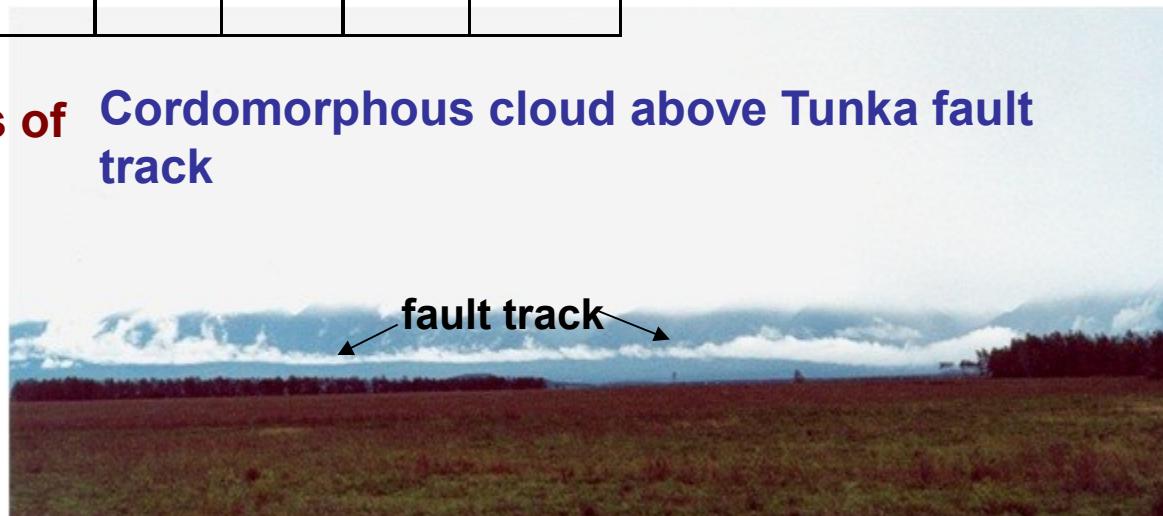
Fault	geochim. flows, kg/km ² · year						SHF, MW _T	F dep, MW _T
	As	Tl	Hg	Ag	Mo	Ge		
Tunka	3.252	0.226	0.020	0.089	0.189	не оп	707.84	323.37
Bargoozin	0.879	0.139	0.013	не оп	не оп	не оп	587.19	362.14
Border zone	1.671	0.229	0.037 0.055	0.018	0.139	не оп	708.09	289.62
Thermal zone Kucheger	21.44	0.413	0.021	0.479	не оп	7.267	74 W _T /M 2	9.553 MW

Surface ionization level of near ground air for Tunka fault track



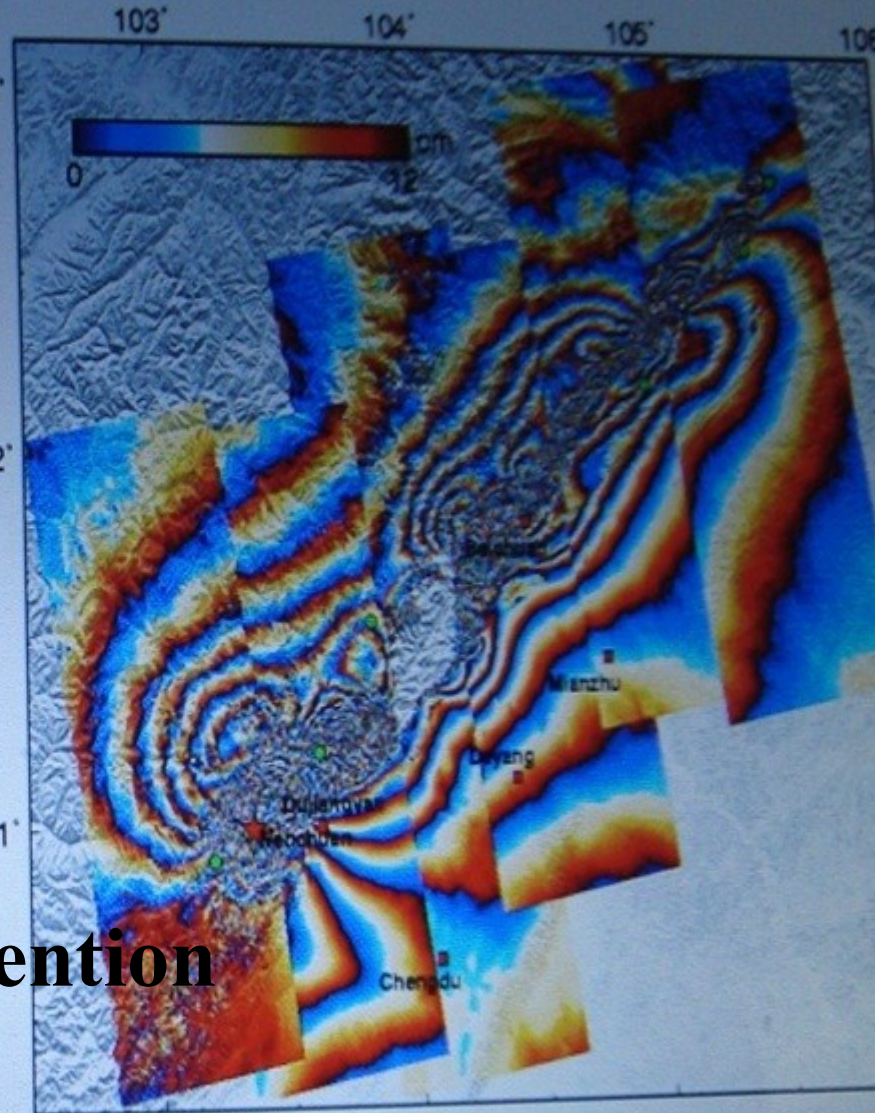
Geochemical flows of large seismoactive regional faults of BRZ

Cordomorphous cloud above Tunka fault track



Affected by Ionosphere

Ionosphere Free



Thank's a lot for Your attention

Ionospheric perturbations above large seismoactive fault, associated with Wenchuan Mw=8.0 earthquake on 12 May 2008 in Sichuan, China (after Xiao-Li Ding)